REDUCING BLOCKING ARTIFACTS IN COMPRESSED IMAGES VIA TRANSFORM-DOMAIN NON-LOCAL COEFFICIENTS ESTIMATION

Xinfeng Zhang[1,2], Ruiqin Xiong[3], Siwei Ma[3], Wen Gao[3]
[1]Key Lab of Intelligent Information Processing, Institute of Computing Technology, Chinese Academy of Sciences, Beijing 100190, China
[2]Graduate University of Chinese Academy of Sciences, Beijing 100049, China
[3]Institute of Digital Media, Peking University, Beijing 100871, China
{xfzhang, rqxiong, swma, wgao}@jdl.ac.cn

ABSTRACT

Block transform coding using discrete cosine transform is the most popular approach for image compression. However, many annoying blocking artifacts are generated due to coarse quantization on transform coefficients independently. This paper proposes an effective blocking artifacts reduction method by estimating the transform coefficients from their quantized version. In the proposed scheme, we estimate the transform coefficients based on an image statistic model and non-local similarity among blocks in transform domain. The parameters used in our proposed scheme are discussed and adaptively selected. Extensive experimental results show that our proposed method significantly reduces blocking artifacts and improves the subjective and the objective quality of block transform coded images.

Index Terms—Block transform coding, Quantization noise, Blocking artifacts, Structure similarity, Non-local similarity

1. INTRODUCTION

Block discrete cosine transform (BDCT) is widely adopted in the existing image and video compression standards, such as JPEG, MPEG-1/2/4 and H.261/263/264, to exploit the spatial correlation among neighboring pixels. In a typical BDCT coding scheme, input image is firstly divided into small blocks, transformed using discrete cosine transform, quantized and entropy coded individually for each block. Quantization maps transform coefficients with a wider range into a quantized value to achieve bit reduction in representing original signal [1] and it is the sole source of coding artifacts. At low bit rate, the quantization step is usually so large that for each block only DC and few AC coefficients are retained. The negative effect is loss of correlation between adjacent blocks and discontinuities on boundaries of blocks [2-3]. As a consequence, reconstructed images suffer from annoying visual effects known as blocking artifacts.

There are two main categories of blocking artifacts reduction techniques in spatial and transform domain, respectively. In [4], Reeve et al. apply a 3×3 Gaussian filter to pixels around block boundaries in order to smooth out the blocking artifacts. However, due to the low-pass nature of spatially invariant Gaussian filter, this method may blur the true edges or texture details near block boundaries in images. To avoid undesirable over-smoothing of coded images, M. Karczewicz et al. [5] employed coding mode and quantization step to select suitable filters. But this method is limited with a special coding method, (e.g. H.264/AVC). A. Zakhor et al. [6-7] take advantage of the quantization intervals of transform coefficients as a convex set to limit the filtering strength based on the theory of projections onto convex sets (POCS). In [8], Stevenson et al. proposed the *maximum a posteriori* (MAP) estimation of the original image using Bayesian rule, employing Huber-Markov random field (Huber-MRF) as the image model. Since the blocking artifacts are caused by the quantization of the transform coefficients independently, some works tackle the problem in the transform domain [9-10]. Chen et al.[9] apply a low pass filter to the DCT coefficients of neighboring blocks. Although adaptively chosen, the filter remains constant with respect to all DCT sub-bands, which is essentially equivalent to applying this low pass filter in spatial domain. Choy et al. [10] estimate the original DCT coefficients from the quantized ones with its local mean and variance. Therefore, filter in [10] is adaptive based on the statistics of different DCT sub-bands.

In this paper, we propose a novel scheme to acquire the *maximum a posteriori* (MAP) estimation of original DCT coefficients under Bayesian framework. In our scheme, the DCT coefficients for each band are adaptively estimated according to an image prior model and a quantization noise model. For image prior model, we assume the local similarity of neighboring blocks' coefficients in each transform sub-band. In order to improve the rationality of image prior model and the efficiency of blocking reduction, we proposed to assign a weight for each sample block in neighborhood by comparing its DCT coefficients with those in current block to be estimated. For quantization noise, we assume it as Gaussian noise for each band. In order to make

978-0-7695-4711-4/12 $26.00 © 2012 IEEE
DOI 10.1109/ICME.2012.159

the scheme more applicable, an effective parameter selection method is also proposed based on extensive statistics results. Finally, the scheme is conducted on overlapped blocks to further decrease the quantization noise.

The remainder of this paper is organized as follows. In section 2, we first formulate blocking reduction as a *maximum a posteriori* estimation problem under Bayesian framework, and then probability distribution models and the calculation of sample weight for image priori model are described in detail. Finally, the closed-form optimization solution for our proposed scheme is derived. In section 3, an effective parameter selection method is introduced based on statistics results. In section 4, experimental results and comparative study is illustrated. Section 5 summaries and concludes this paper.

2. DEBLOCKING WITH VALIDITY SIMILARITY

2.1. Problem Formulation

Suppose an image $\boldsymbol{I}$ of size $H\times W$, where $\boldsymbol{I}(i, j)$ denotes a pixel in the image $\boldsymbol{I}$ and the indices i and j are the coordinates in the vertical and the horizontal directions, respectively. The size of discrete cosine transform (DCT) used for image coding is $M\times M$. we use $\boldsymbol{B}_{m,n}(i, j)$ to denote a $M\times M$ block in $\boldsymbol{I}$, with its top left pixel being $\boldsymbol{I}(m, n)$. To be specific, the pixels in this block are

$$\boldsymbol{B}_{m,n}(i,j) = \boldsymbol{I}(m+i, n+j),\ i, j = 0, 1,\ldots, M\text{-}1 \tag{1}$$

We use $\mathbf{x}$ to represent the original data (i.e. pixel intensity) of image $\boldsymbol{I}$ and use $\mathbf{x}_{\boldsymbol{B}}(i,j)$, $i, j = 0, 1,\ldots, M$-1 and $\mathbf{X}_{\boldsymbol{B}}(u,v)$, $u,v= 0, 1,\ldots, M$ -1 to represent the data and the transform coefficients of a block $\boldsymbol{B}$, respectively. $\mathbf{X}$ is the original image in DCT domain made up of $\mathbf{X}_{\boldsymbol{B}}(u,v)$. We call $\mathbf{x}_{\boldsymbol{B}}$ and $\mathbf{X}_{\boldsymbol{B}}$ data-block and transform-block of $\boldsymbol{B}$, respectively. The DCT is denoted as $\mathbf{T}$, then $\mathbf{X}_{\boldsymbol{B}} = \mathbf{T}\mathbf{x}_{\boldsymbol{B}}$. These transform coefficients $\mathbf{X}_{\boldsymbol{B}}$ are then scalar quantized according to a quantization matrix $\boldsymbol{Q}$ and $\boldsymbol{Q}(u,v)$ represents the quantization step for the corresponding sub-band (u,v), $u, v = 0, 1,\ldots,M$-1. The forward and inverse quantization can be illustrated in (2) and (3), respectively.

$$\mathbf{I}_{\boldsymbol{B}}(u,v) = \boldsymbol{F}^{\boldsymbol{Q}}\left(\mathbf{X}_{\boldsymbol{B}}(u,v)\right) = round\left(\frac{\mathbf{X}_{\boldsymbol{B}}(u,v)}{\boldsymbol{Q}(u,v)}\right) \tag{2}$$

$$\mathbf{Y}_{\boldsymbol{B}}(u,v) = \boldsymbol{Q}(u,v)\cdot\mathbf{I}_{\boldsymbol{B}}(u,v) \tag{3}$$

Here $\mathbf{I}_{\boldsymbol{B}}(u,v)$ is the index of quantization interval and $\mathbf{Y}_{\boldsymbol{B}}$ is the reconstruction value in that interval. The function, $round(x)$, rounds x to the nearest integer. Therefore, blocking reduction can be regards as a MAP estimation problem based on the following assumption:

$$\mathbf{Y}_{\boldsymbol{B}} = \mathbf{X}_{\boldsymbol{B}} + \mathbf{N}_{\boldsymbol{B}} \tag{4}$$

In equation (4), $\mathbf{N}_{\boldsymbol{B}}$ is the quantization noise for a block. Then the MAP estimator for the original transform coefficients is given as follows,

$$\hat{\mathbf{X}}_{\boldsymbol{B}} = \underset{\mathbf{X}_{\boldsymbol{B}}}{\operatorname{argmax}} \Pr\left(\mathbf{X}_{\boldsymbol{B}} \middle| \mathbf{Y}_{\boldsymbol{B}}, \boldsymbol{B}\in\Omega\right) \tag{5}$$

$$\Omega = \left\{\boldsymbol{B}_{m,n} \middle| 0 \le m < H-M, 0 \le n < W-M\right\} \tag{6}$$

Applying the Bayesian rule and taking logarithm, the problem in (5) is transformed to the following problem,

$$\hat{\mathbf{X}}_{\boldsymbol{B}} = \underset{\mathbf{X}_{\boldsymbol{B}}}{\operatorname{argmax}} \log\Pr\left(\mathbf{Y}_{\boldsymbol{B}} \middle| \mathbf{X}_{\boldsymbol{B}}, \boldsymbol{B}\in\Omega\right) + \log\Pr\left(\mathbf{X}_{\boldsymbol{B}}\right) \tag{7}$$

In problem (7), $\Pr(\mathbf{Y}_{\boldsymbol{B}}|\ \mathbf{X}_{\boldsymbol{B}},\ \boldsymbol{B}\in\Omega)$ represents the conditional probability of the decompressed coefficients $\mathbf{Y}_{\boldsymbol{B}}$ when the original transform coefficients is given, and $\Pr(\mathbf{X}_{\boldsymbol{B}})$ is *a priori* probability of the original transform coefficients. The two probability distributions will be illustrated in next subsection.

Note that the interval of the original transform coefficients is available at the decoder based on the quantization matrix. Therefore, the MAP estimator should not exceed the interval constrained by quantization matrix and the MAP estimation can be formulated as follows finally.

$$\hat{\mathbf{X}}_{\boldsymbol{B}} = \underset{\mathbf{X}_{\boldsymbol{B}}}{\operatorname{argmax}} \left\{log\Pr\left(\mathbf{Y}_{\boldsymbol{B}} \middle| \mathbf{X}_{\boldsymbol{B}}, \boldsymbol{B}\in\Omega\right) + log\Pr\left(\mathbf{X}_{\boldsymbol{B}}\right)\right\} \tag{8}$$

$$\begin{aligned} s.t.\quad & \hat{\mathbf{X}}_{\boldsymbol{B}}(u,v) \in \left[\mathbf{Y}_{\boldsymbol{B}}^{\min}(u,v), \mathbf{Y}_{\boldsymbol{B}}^{\max}(u,v)\right], \text{ for all } \boldsymbol{B}\in\Omega \\ & \mathbf{Y}_{\boldsymbol{B}}^{\min}(u,v) = \mathbf{Y}_{\boldsymbol{B}}(u,v) - \frac{1}{2}\boldsymbol{Q}(u,v), \\ & \mathbf{Y}_{\boldsymbol{B}}^{\max}(u,v) = \mathbf{Y}_{\boldsymbol{B}}(u,v) + \frac{1}{2}\boldsymbol{Q}(u,v) \end{aligned} \tag{9}$$

2.2. Probability Distribution Model

For the conditional probability in (8), we assume that the quantization noise is uncorrelated with $\mathbf{X}_{\boldsymbol{B}}(u,v)$. Then we substitute (4) into the conditional probability.

$$\Pr\left(\mathbf{Y}_{\boldsymbol{B}} \middle| \mathbf{X}_{\boldsymbol{B}}\right) = \Pr\left(\mathbf{X}_{\boldsymbol{B}} + \mathbf{N}_{\boldsymbol{B}} \middle| \mathbf{X}_{\boldsymbol{B}}\right) = \Pr\left(\mathbf{N}_{\boldsymbol{B}} \middle| \mathbf{X}_{\boldsymbol{B}}\right) = \Pr\left(\mathbf{N}_{\boldsymbol{B}}\right) \tag{10}$$

In addition, we assume the quantization noise follows Gaussian distribution at each sub-band [11]. For simplicity, the variance of the conditional probability for each band in (8) is calculated by the following equation.

$$\sigma_N^2(u,v) = \frac{1}{12}\boldsymbol{Q}^2(u,v) \tag{11}$$

Therefore, the conditional probability density function is formulated as follows.

$$\begin{aligned} & \Pr\left(\mathbf{Y}_{\boldsymbol{B}} \middle| \mathbf{X}_{\boldsymbol{B}}, \boldsymbol{B}\in\Omega\right) \\ & = \Pr(\mathbf{N}) \\ & = \frac{1}{(2\pi)^{M/2}\left|\mathbf{R}_{\mathbf{N}}\right|^{1/2}} exp\left\{-\frac{1}{2}\left(\mathbf{X}_{\boldsymbol{B}} - \mathbf{Y}_{\boldsymbol{B}}\right)^T \mathbf{R}_{\mathbf{N}}^{-1}\left(\mathbf{X}_{\boldsymbol{B}} - \mathbf{Y}_{\boldsymbol{B}}\right)\right\} \\ & = \frac{1}{(2\pi)^{M/2}\left|\mathbf{R}_{\mathbf{N}}\right|^{1/2}} exp\left\{-\frac{1}{2}\sum_{v}^{M}\sum_{u}^{M}\frac{\left(\mathbf{X}_{\boldsymbol{B}}(u,v) - \mathbf{Y}_{\boldsymbol{B}}(u,v)\right)^2}{\sigma_{\mathbf{N}}^2(u,v)}\right\} \end{aligned} \tag{12}$$

where $\mathbf{R}_{\mathbf{N}}$ is a diagonal matrix and diagonal elements consist of $\sigma_{\mathbf{N}}^2$.

For the priori probability in (8), we assume that the transform coefficients are piecewise stationary, and then a priori distribution of coefficients in each quantization

interval is also assumed as Gaussian distribution [10]. In other words, the statistical characteristics of transform coefficients are similar for neighboring blocks. Therefore, to infer the coefficients of a certain block, we use the coefficients from its neighboring blocks as extra samples to form the priori distribution. For any block $\boldsymbol{B}_{m,n}$, we define the set of its neighboring blocks (in a $(2L+1)\times(2L+1)$ window) as

$$\mathcal{N}_L(\boldsymbol{B}_{m,n}) = \{\boldsymbol{B}_{k,l} \,|\, m-L \le k \le m+L, n-L \le l \le n+L\} \setminus \{\boldsymbol{B}_{m,n}\} \quad (13)$$

Then the priori probability in (8) used Gaussian distribution is formulated in (14)-(16)

$$\begin{aligned} \Pr(\mathbf{X}_{\boldsymbol{B}}) &= \frac{1}{(2\pi)^{M/2}\left|\mathbf{R}_{\mathcal{N}_L}\right|^{1/2}} exp\left\{-\frac{1}{2}\left(\mathbf{X}_{\boldsymbol{B}}-\bar{\mathbf{Y}}_{\mathcal{N}_L}\right)^T \mathbf{R}_{\mathcal{N}_L}^{-1}\left(\mathbf{X}_{\boldsymbol{B}}-\bar{\mathbf{Y}}_{\mathcal{N}_L}\right)\right\} \\ &= \frac{1}{(2\pi)^{M/2}\left|\mathbf{R}_{\mathcal{N}_L}\right|^{1/2}} exp\left\{-\frac{1}{2}\sum_{u}^{M}\sum_{v}^{M}\frac{\left(\mathbf{X}_{\boldsymbol{B}}(u,v)-\bar{\mathbf{Y}}_{\mathcal{N}_L}(u,v)\right)^2}{\sigma^2_{\mathcal{N}_L}(u,v)}\right\} \end{aligned} \quad (14)$$

$$\bar{\mathbf{Y}}_{\mathcal{N}_L}(u,v) = \frac{1}{|\mathcal{N}_L|}\sum_{i}^{|\mathcal{N}_L|}\mathbf{Y}^i_{\boldsymbol{B}}(u,v) \quad (15)$$

$$\sigma^2_{\mathcal{N}_L}(u,v) = \frac{1}{|\mathcal{N}_L|}\sum_{i}^{|\mathcal{N}_L|}\left(\mathbf{Y}^i_{\boldsymbol{B}}(u,v)-\bar{\mathbf{Y}}_{\mathcal{N}_L}(u,v)\right)^2 \quad (16)$$

Here, $\sigma^2_{\mathcal{N}_L}(u,v)$ is the variance of DCT coefficients in sub-band (u,v) extracted from these neighboring samples and $|\mathcal{N}_L|$ is the number of samples in the neighborhood.

2.3. Sample Weight

In the above discussion, we assume that transform coefficients are piecewise stationary in the neighborhoods and follow Gaussian distribution model. Here, we denote this assumption as *stationary assumption*. In (15)-(16), equal weight is assigned for each sample based on the assumption. However, this assumption is not valid for some areas in an image, especially for edge or texture regions which are different from the current block to be estimated distinctly. Therefore, in order to make the rationality of *stationary assumption* and improve the efficiency of blocking reduction, we assign a weight for each sample in the given neighborhood to measure its similarity with the original block $\mathbf{X_B}$ in the center of neighborhood (described in (13)). The sum square difference (SSD) of transform coefficients between sample bock and original center block is employed to measure their similarity. Because the original block $\mathbf{X}_{\boldsymbol{B}}$ is unknown, we use the reconstructed block $\mathbf{Y}_{\boldsymbol{B}}$ of $\mathbf{X}_{\boldsymbol{B}}$ instead. The *sample weight* for $\mathbf{Y}_{\boldsymbol{Bi}}$ can be illustrated as follows.

$$w_{\boldsymbol{Bi}} = \frac{1}{Z} exp\left(-\frac{\left\|\mathbf{Y}_{\boldsymbol{Bi}}-\mathbf{Y}_{\boldsymbol{B}}\right\|^2}{h}\right) \quad (17)$$

$$Z = \sum_{i=1}^{|\mathcal{N}_L(\boldsymbol{B})|} exp\left(-\frac{\left\|\mathbf{Y}_{\boldsymbol{Bi}}-\mathbf{Y}_{\boldsymbol{B}}\right\|^2}{h}\right), \quad \boldsymbol{Bi} \in \mathcal{N}_L(\boldsymbol{B})$$

The mean and variance of neighboring blocks are calculated with sample weight instead of (15) and (16).

$$\bar{\mathbf{Y}}_{\mathcal{N}_L}(u,v) = \sum_{i}^{|\mathcal{N}_L|} w_i(u,v)\,\mathbf{Y}^i_{\boldsymbol{B}}(u,v) \quad (18)$$

$$\sigma^2_{\mathcal{N}_L}(u,v) = \sum_{i}^{|\mathcal{N}_L|} w_i(u,v)\left(\mathbf{Y}^i_{\boldsymbol{B}}(u,v)-\bar{\mathbf{Y}}_{\mathcal{N}_L}(u,v)\right)^2 \quad (19)$$

Here, the *sample weight* is the same for all the sub-bands in sample $\mathbf{Y}_{\boldsymbol{Bi}}$. h is a smoothness factor to control the distribution of the sample weights and it also affects the final estimation accuracy for the original coefficients. This *sample weight* is not only depresses the negative effects of *stationary assumption*, but it also extends from local to non-local stationary assumption.

2.4. Optimization Solution

The problem in (8) is a convex optimization. The optimization solution is acquired by making derivation of (8) equal 0, which is formulated as follows.

$$\begin{aligned} &\frac{\partial log\Pr(\mathbf{Y}_{\boldsymbol{B}}|\mathbf{X}_{\boldsymbol{B}})}{\partial \mathbf{X}_{\boldsymbol{B}}} + \frac{\partial log\Pr(\mathbf{X}_{\boldsymbol{B}})}{\partial \mathbf{X}_{\boldsymbol{B}}} \\ &= \frac{\partial\left(-\frac{1}{2}(\mathbf{X}_{\boldsymbol{B}}-\mathbf{Y}_{\boldsymbol{B}})^T\mathbf{R}_{\mathbf{N}}^{-1}(\mathbf{X}_{\boldsymbol{B}}-\mathbf{Y}_{\boldsymbol{B}})\right)}{\partial \mathbf{X}_{\boldsymbol{B}}} \\ &\quad + \frac{\partial\left(-\frac{1}{2}\left(\mathbf{X}_{\boldsymbol{B}}-\bar{\mathbf{Y}}_{\mathcal{N}_L}\right)^T\mathbf{R}_{\mathcal{N}_L}^{-1}\left(\mathbf{X}_{\boldsymbol{B}}-\bar{\mathbf{Y}}_{\mathcal{N}_L}\right)\right)}{\partial \mathbf{X}_{\boldsymbol{B}}} \\ &= -\left(\mathbf{R}_{\mathcal{N}_L}^{-1}+\mathbf{R}_{\mathbf{N}}^{-1}\right)\mathbf{X}_{\boldsymbol{B}} + \mathbf{R}_{\mathbf{N}}^{-1}\mathbf{Y}_{\boldsymbol{B}} + \mathbf{R}_{\mathcal{N}_L}^{-1}\bar{\mathbf{Y}}_{\mathcal{N}_L} = 0 \end{aligned} \quad (20)$$

Therefore, the closed-form solution of MAP estimation in (8) is illustrated in (21)-(23). In (23), we project the MAP estimator $\hat{\mathbf{X}}_{\boldsymbol{B}}$ into the quantization interval.

$$\hat{\mathbf{X}}_{\boldsymbol{B}} = \left(\mathbf{R}_{\mathcal{N}_L}^{-1}+\mathbf{R}_{\mathbf{N}}^{-1}\right)^{-1}\mathbf{R}_{\mathbf{N}}^{-1}\mathbf{Y}_{\boldsymbol{B}} + \left(\mathbf{R}_{\mathcal{N}_L}^{-1}+\mathbf{R}_{\mathbf{N}}^{-1}\right)^{-1}\mathbf{R}_{\mathcal{N}_L}^{-1}\bar{\mathbf{Y}}_{\mathcal{N}_L} \quad (21)$$

$$\hat{\mathbf{X}}_{\boldsymbol{B}}(u,v) = \frac{\sigma^2_{\mathcal{N}_L}(u,v)}{\sigma^2_{\mathbf{N}}(u,v)+\sigma^2_{\mathcal{N}_L}(u,v)}\mathbf{Y}_{\boldsymbol{B}}(u,v) + \frac{\sigma^2_{\mathbf{N}}(u,v)}{\sigma^2_{\mathbf{N}}(u,v)+\sigma^2_{\mathcal{N}_L}(u,v)}\bar{\mathbf{Y}}_{\mathcal{N}_L}(u,v) \quad (22)$$

$$\hat{\mathbf{X}}_{\boldsymbol{B}}(u,v) = \begin{cases} \mathbf{Y}^{\min}_{\boldsymbol{B}}(u,v), & \text{if } \hat{\mathbf{X}}_{\boldsymbol{B}}(u,v) < \mathbf{Y}^{\min}_{\boldsymbol{B}}(u,v) \\ \hat{\mathbf{X}}_{\boldsymbol{B}}(u,v), & \text{if } \mathbf{Y}^{\min}_{\boldsymbol{B}}(u,v) \le \hat{\mathbf{X}}_{\boldsymbol{B}}(u,v) \le \mathbf{Y}^{\mathbf{max}}_{\boldsymbol{B}}(u,v) \\ \mathbf{Y}^{\mathbf{max}}_{\boldsymbol{B}}(u,v), & \text{if } \hat{\mathbf{X}}_{\boldsymbol{B}}(u,v) > \mathbf{Y}^{\mathbf{max}}_{\boldsymbol{B}}(u,v) \end{cases} \quad (23)$$

3. ADAPTIVE PARAMETER SELECTION

In our proposed scheme, two parameters need to be provided, local window size L in (13) and the smoothness factor h in (17). In order to acquire best parameters, we first fixed the local window size L =5 and search the best smoothness factor h for images include *Airplane*, *Barbara*, *Cameraman*, *Cap*, *Elaine*, *Fishingboat*, *Lena*. We try out smoothness factor from 5 to 60 with increment 5 for all the JPEG coded images with quality factor (*QF*) set to 10, 15, 20… 40. Fig.1 shows the relationship between the best smoothness factor (in vertical axis) and average quantization step of quantization matrix Q (in horizontal axis). From Fig.1, we can see that the smoothness factor h decreases along with quantization step decreasing. Therefore, we use the average of all quantization steps in quantization matrix Q, denoted as Q_{Avg}, to predict best parameter h. The approximate relationship between Q_{Avg} and h can be

estimated by linear regression, illustrated in following.

$$h = 0.095Q_{Avg} + 19.60 \quad (24)$$

In order to find the best local window size L in (13), we try out different window size L from 1 to 10 with best smoothness factor given in (24). Fig.2 illustrates the relationship between window size L and performance of our proposed scheme at different compression rates. The horizontal ordinate represents the window size, and the vertical ordinate represents the performance of our proposed scheme. We can see that our proposed scheme achieves best performance when window size is set 7 for many images. Due to limited space, only the results of two images are illustrated in Fig.2. At the same time, compression rate have little impact on window size comparing Fig.2 (a) and (b). Therefore, we set the local window size as 7 for our proposed scheme.

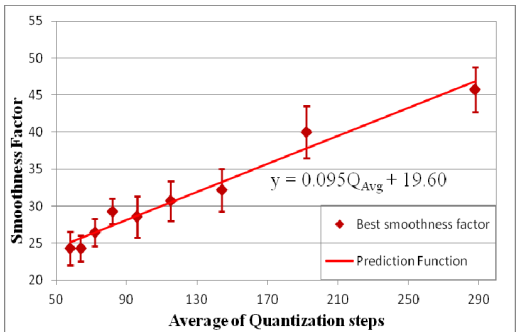

Fig.1: the distribution of best smoothness factor h for the test images with different quantization steps.

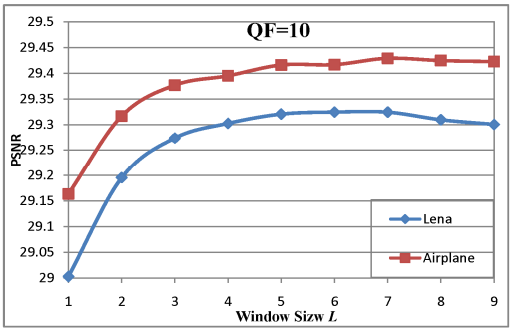

(a)

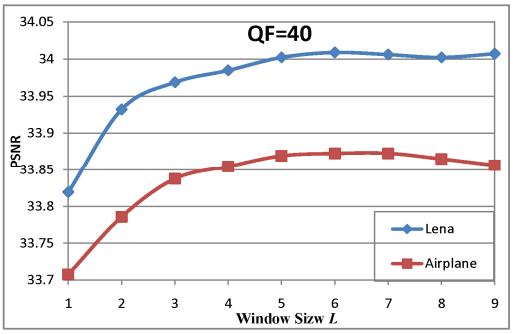

(b)

Fig.2: The relationship between local window size L and the performance of our proposed scheme. (a) Images coed with quality factor 10. (b) Images coded with quality factor 40.

4. EXPERIMENTAL RESULTS

In this section, we evaluate the performance of the proposed scheme. We use the popular *Lena*, *Barbara*, *Elaine*, *Peppers*, *Fishboat, Cameraman* and the Kodak image set as the test images, listed in Table 1-2. These images are coded by a JPEG coder [12] with quality factor (*QF*) set to 10, 15, 20,…, 50, and then reconstructed using standard JPEG decoder [12], the SPL scheme [10], the nonlocal means filter (NLM) [13] and the proposed scheme. The parameter of smoothness factor h used in our proposed method is adaptively set based on equation (24) and local window size is set 7. The PSNR results for *QF* = 10 and *QF* = 40 (a low quality and a medium quality) are summarized in Table 1-2. We can see that the proposed scheme achieves 1.16dB, 0.84dB and 0.31dB gain over the standard JPEG decoder, the SPL scheme and NLM scheme with *QF* =10 on average, respectively. When *QF* is set 40, our proposed scheme still achieves 1.05dB, 0.75dB and 0.72dB gain over JPEG decoder, the SPL and NLM scheme. It achieves up to 1.64 dB gain over JPEG decoder for *Elaine* with *QF* = 10.

Table 1 PSNR quality (in dB) of restored images using different methods for test images compressed with *QF* = 10.

Image	JPEG	SPL	NLM	Proposed
Airplane	28.47	28.61	29.15	29.44
Barbara	27.60	27.90	28.39	28.64
Cameraman	26.44	26.59	26.98	27.36
Cap	29.74	30.20	30.77	31.00
Elaine	29.52	29.97	30.82	31.16
Fishboat	26.37	26.66	26.98	27.31
Lena	28.02	28.38	29.01	29.34
Parrot	29.62	30.08	30.51	30.83
Peppers	28.39	28.68	29.39	29.87
Girl	28.73	29.09	29.55	29.73
Sailboats	28.26	28.59	29.05	29.42
Sailboats2	28.21	28.53	29.00	29.18
Window	27.42	27.66	28.24	28.47
Average	28.21	28.53	29.06	29.37

Table 2 PSNR quality (in dB) of restored images using different methods for test images compressed with *QF* = 40.

Image	JPEG	SPL	NLM	Proposed
Airplane	32.87	33.11	33.03	33.87
Barbara	31.56	31.94	32.06	32.55
Cameraman	30.89	31.14	30.76	31.87
Cap	33.91	34.17	34.48	34.87
Elaine	34.53	34.85	35.24	35.79
Fishboat	31.12	31.48	31.20	32.13
Lena	32.70	33.14	33.18	34.04
Parrot	34.63	34.95	34.71	35.66
Peppers	33.50	33.72	33.95	34.83
Girl	32.85	33.18	33.23	33.74
Sailboats	33.22	33.52	33.58	34.25
Sailboats2	32.68	32.97	32.99	33.63
Window	32.02	32.32	32.46	33.01
Average	32.81	33.11	33.14	33.86

Fig.3 shows how the reconstruction quality and the improvement vary with JPEG quality factor. From Fig.3, we can see that the proposed scheme works well over a large quality (or bit rate) range. The PSNR improvement over the standard JPEG decoder and the SPL algorithm are similar for all the tested *QF* settings. Our proposed scheme achieves higher gain over the NLM at high bit rate. This is because NLM is a spatial filter without quantization constrain. At low bit rate (large quantization step), the quantization constrain is loose and its influence is insignificant. However, at higher bit rate (small quantization step), the quantization constrain is close and it plays an important role on preventing over-smoothing.

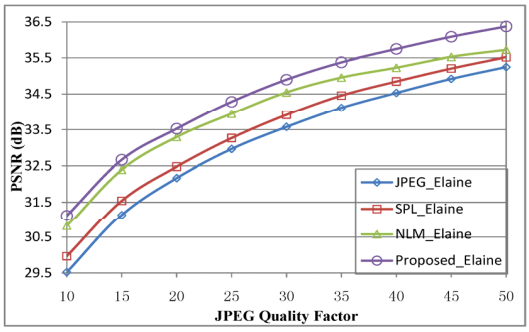

(a)

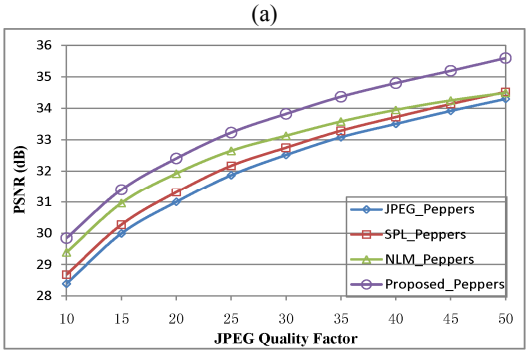

(b)

Fig.3: The reconstruction PSNR (in dB) with different JPEG quality factors for the JPEG decoder, SPL [10], NLM [13] and the proposed scheme.

In Fig.4 and Fig.5, we show the subjective quality of reconstructed images. Fig.4 shows the results of *Elaine* compressed using *QF* = 15 and Fig.5 shows the results of *Lena* compressed using *QF* = 40. The blocking artifacts are very obvious in the standard JPEG decoded image. Such artifacts are partially reduced by the SPL scheme, but some blocking artifacts remained in the image are still observed. The NLM scheme is remove almost all the blocking artifacts, but it also blurring the image details, especially in Fig.5 with *QF*=40. Our proposed scheme removes most of the blocking artifacts while persevering image details. From Fig. 5, we can see that the NLM method smoothes most textures of hat, which are well preserved in our proposed scheme.

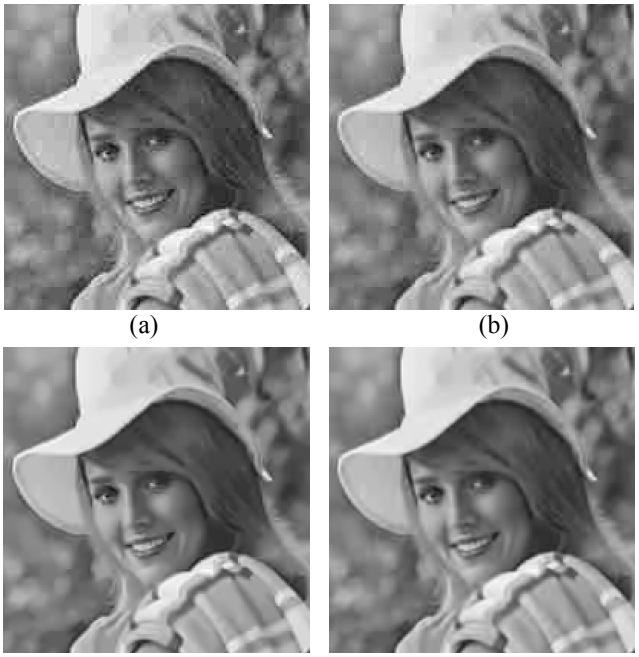

(a) (b) (c) (d)

Fig.4: The reconstruction *Elaine* with different methods (*QF*=15), (a) JPEG decoder, (b) SPL [10], (c) NLM [13], (d) Proposed scheme.

(a) (b) (c) (d)

Fig.5: The reconstruction *Lena* with different methods (*QF*=40), (a) JPEG decoder, (b) SPL [10], (c) NLM [13], (d) Proposed scheme.

5. CONCLUSION

In this paper, we propose a new transform-domain approach for blocking artifacts reduction. In the proposed scheme, the

transform coefficients of a compressed image are restored from a *maximum a posteriori* estimation. The quality improvement of restored images is improved mainly from four aspects. First, an image prior model, that assumes local similarity of the neighboring blocks' coefficients in each sub-band, is able to smooth the discontinuity around block boundaries efficiently. Second, sample weight is proposed to measure blocks' similarity, which is able to depress the negative effects when the local similarity assumption is invalid. Third, a practical adaptive parameter selection method is proposed and it improves the practicability and estimation accuracy. Finally, the quantization constrain prevents MAP estimation over-smoothing and guarantee our proposed scheme efficient among a large range of compression rate. Experimental results demonstrated that the proposed approach can remarkably improve both the subjective and the objective quality of the block transform coded images.

6. ACKNOWLEDGEMENTS

This work was supported by National Science Foundation of China (61121002, 61073083, 61103088 and 60833013), National Basic Research Program of China (973 Program, 2009CB320904), Beijing Natural Science Foundation (4112026), and Specialized Research Fund for the Doctoral Program of Higher Education (20100001120027).

7. REFERENCES

[1] X. Jin, S. Life and K. N. Ngan, "Composite Model-Based DC Dithering for Suppressing Contour Artifacts in Decompressed Video," IEEE Transactions on Image Processing, vol. 20, no. 8, Aug. 2011.

[2] S. D. Kim, J. Yi, H. M. Kim, and J. B. Ra, "A deblocking filter with two separate modes in block-based video coding," IEEE Transactions on Circuits and Systems for Video Technology, vol. 9, pp. 156–160, Feb. 1999.

[3] Y.-L. Lee and H. W. Park, "Loop filtering and post-filtering for low-bit rates moving picture coding," Signal Processing: Image Communication, vol.16, pp. 871–890, 2001.

[4] H. C. Reeve III and J. S. Lim, "Reduction of blocking effect in image coding," IEEE International Conference on Acoustics, Speech, and Signal Processing, vol. 8, pp. 1212–1215, April 1983.

[5] P. List, A. Joch, J. Lainema, G. Bjøntegaard and M. Karczewicz, "Adaptive Deblocking Filter," IEEE Transactions on Circuits and Systems for Video Technology, vol.13, no.7, Jul. 2003.

[6] A. Zakhor, "Iterative procedures for reduction of blocking effects in transform image coding," IEEE Transactions on Circuits and Systems for Video Technology, vol. 2, no. 1, pp. 91–95, Mar 1992.

[7] Y. Yang, N.P. Galatsanos, and A.K. Katsaggelos, "Regularized reconstruction to reduce blocking artifacts of block discrete cosine transform compressed images," IEEE Transactions on Circuits and Systems for Video Technology, vol. 3, no. 6, pp. 421–432, Dec 1993.

[8] T. P. O'Rourke and R. L. Stevenson, "Improved image decompression for reduced transform coding artifacts," IEEE Transactions on Circuits and Systems for Video Technology, vol. 5, no. 6, pp. 490–499, Dec 1995.

[9] T. Chen, H. R. Wu, and B. Qiu, "Adaptive postfiltering of transform coefficients for the reduction of blocking artifacts," IEEE Transactions on Circuits and Systems for Video Technology, vol. 11, no. 5, pp. 594–602, May 2001.

[10] S. S. O. Choy, Y.-H. Chan, and W.-C. Siu, "Reduction of block-transform image coding artifacts by using local statistics of transform coefficients," IEEE Signal Processing Letters, vol. 4, no. 1, pp. 5–7, Jan 1997.

[11] D. Sun and W.-K. Chan, "Postprocessing of Low Bit-Rate Block DCT Coded Images Based on a Fields of Experts Prior," IEEE Transactions on Image Processing, vol. 16, no. 11, pp.2743-2751, Nov. 2007.

[12] JPEG software is available from: http://www.ijg.org/.

[13] A. Buades, B. Coll, and J. M. Morel, "A review of image denoising algorithms, with a new one," SIAM Journal on Multiscale Modeling and Simulation, vol. 4, no. 2, pp. 490–530, 2005.